3D Natural State Model of Menengai East Geothermal Reservoir, Kenya.

Marietta W. Mutonga and Yasuhiro Fujimitsu

[1] Department of Earth Resources Engineering, Graduate School of Engineering, Kyushu University, Fukuoka 819-0395, Japan/ Geothermal Development Company Ltd, Central Rift P.O.Box 17700, 200100 Nakuru

[2] Department of Earth Resources Engineering, Faculty of Engineering, Kyushu University, Fukuoka 819-0395,Japan.

***Email mariettawa@yahoo.com/mmutonga@gdc.co.ke**

Keywords
The numerical, natural state, Menengai East

ABSTRACT

The Menengai Geothermal field is a high temperature geothermal field located within the Central Kenya Rift. It is located 10 km from Nakuru town the fourth largest city in Kenya and 20 km from Lake Nakuru. Temperatures above 300ºC have been realized in this field where more than 40 wells have been drilled with more than 130 Mwe is ready for evacuation and a 35 Mwe power plant is underway. Within the caldera two major upflow areas have been noted. A large one to the West & Central part of the caldera and a smaller one to the East of the caldera, therefore the field can be divided into two major parts East and West. The Western part of the field is more developed and most of the wells have been drilled in this area. The east is an expansion area for the field, atleast four wells have successfully been drilled in this area hence the need for a 3D Natural state model focused on this area. We have made use surface exploration surveys and the findings derived from drilling, logging, and testing of geothermal wells to build a 3D natural state model of the geothermal system by means of the TOUGH2 reservoir simulator, supported by Petrasim 5.3 graphical interface. The model was run to steady state conditions and calibrated against data obtained from well pressure and temperature profiles recorded under warm-up and flowing conditions, as well as available production test results, the actual pressure and temperature profiles agree to a large extent with the modelled results.

1.0 Introduction

Kenya currently has a population of over 54 million people, and its per-capita energy usage is about 170 kWh, which is significantly higher than that of its neighbors (Tanzania's is 60% higher, and Uganda's is half that). Energy consumption in the nation has been steadily rising, with electrification rates rising from 19% in 2010 to roughly 75% in 2020. Over 85% of the electricity produced in Kenya currently is produced via renewable energy sources. In addition, 89.9% of the electricity used is generated domestically. Fossil fuel consumption has made a significant contribution to climate change, which primarily impacts the most vulnerable. Kenya aims to have

100% renewable energy in its power mix by 2030 to reduce greenhouse gas emissions and obtain carbon credits. Thanks to major capacity additions over the previous ten years, particularly in geothermal, the proportion of renewables in the power mix increased to 95% in 2002. Geothermal energy leads in the energy mix at 48.4%, followed by hydro, wind, thermal, and solar energy. Geothermal energy currently has an installed capacity of 891.8 MWe (Country Energy Report 2020). It comes primarily from Olkaria, the country of Kenya's first geothermal field to be developed. The Menengai geothermal field is the country's second geothermal field, and it is hosted within The Menengai Caldera, a late Quaternary caldera volcano formed on a massive shield volcano located in the inner trough of the Kenya rift valley associated with a high thermal gradient resulting from shallow magmatic intrusions. More than 40 wells have been drilled in the Menengai field because of surface studies that revealed a significant geothermal potential. Temperatures above 300 ^{o} C have also been recorded at depths as shallow as 1600 m and more than 130 MWe has already been realized so far. The project has been carried out in phases. The 1st Phase (105 Mwe) is in the central part of the caldera, which is the main upflow zone is the most developed, with two 35Mwe power plants underway. Since the central part of the caldera has been successfully explored and drilled, there's a need for a step-out strategy. The 2nd Phase is located at the eastern part of the Menengai Caldera, where we have the 2nd upflow(Figure 2), which is expected to generate 60 MW of steam equivalent. The geo-scientific studies and drilling of exploratory wells have already been conducted in this part.

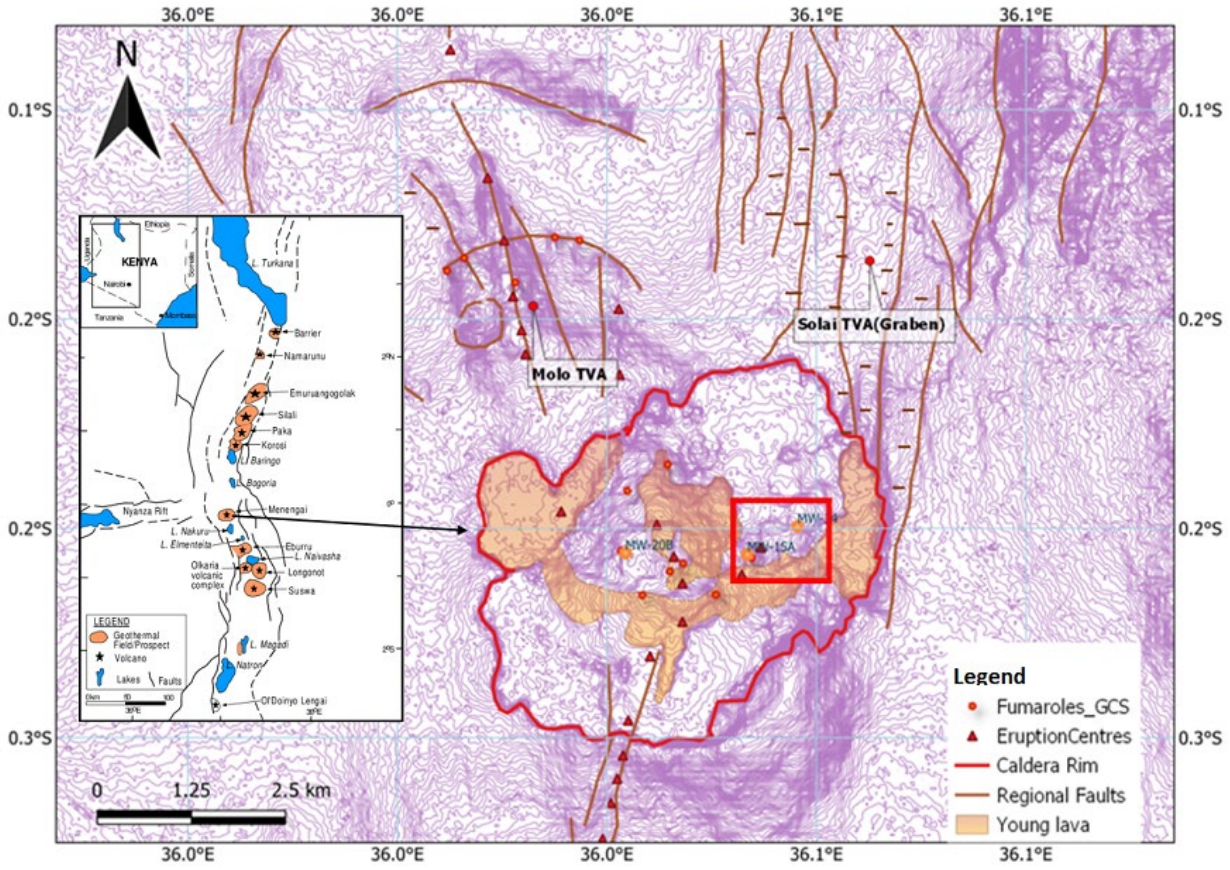

Figure 1: Show the location of the Menengai caldera, Fumaroles, Eruption centers and regional faults, at the center of then caldera is the young lava that emanated from the eruptive fissure running E-W, marked in red is the Natural state modelled area.

Drilling results and related studies indicate that there exists a naturally fractured geothermal reservoir at depths between 700-2100 m that reaches temperatures above 250°C. Surface studies indicate that the area is within an intersection of the Solai and central caldera arcuate structures (Njue and Kipngok 2019). Based on the alteration mineralogy and temperature profiles from MW-15 and MW-18A, we confirm the existence of sufficient heat of more than 300°C.

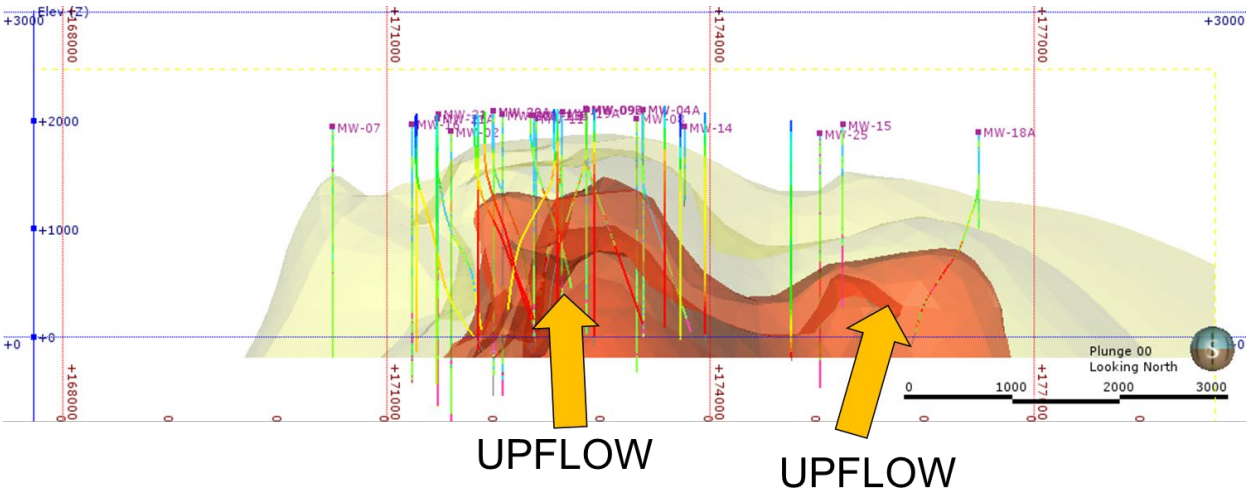

Figure 2:Reservoir temperature model for Menengai geothermal field showing the main up flow and the 2nd up flow zone to the East.

To better understand geothermal system, a conceptual model of the field was constructed as well as a 3 D natural state numerical model. The rock types were assigned to each block in several layers. Initial and boundary conditions were defined according to existing data. Model validation was conducted by matching available downhole temperature and pressure data. To do this, it was necessary to run the models at steady state and compare the simulated data to the known or system's interpreted conditions. The model's attributes, such as permeability, rock density, and so on, were changed in this iterative process until a good match was established.

1.1 Previous Similar Works

Several versions of the numerical model of the geothermal system have been developed over the years. A supercritical model of Menengai was developed and calibrated by O'Sullivan et al., (2015) using the supercritical variant of AUTOUGH2. The model's basic heat flow had to be increased, and some of the deep permeabilities had to be changed, as part of the calibration process. The supercritical model suggested that the identical production scenario would result in about 30% more steam than predicted by the normal model. Much of the field was covered. A 3D Natural state model of the Menenagi Geothermal Field was also created by Montegrossi et al., (2015), however it focused mostly on the central part of the caldera, where most wells had already been drilled.

1.2 Conceptual model of Menengai Geothermal Reservoir

In Menengai observation from surface studies of high temperature field include altered grounds, fumaroles, and eruption centers. Seismic studies by Simiyu and Keller (1997) indicated clusters of shallow microearthquakes under the caldera and relate these to a high-temperature geothermal field associated with shallow magma bodies. A heat loss survey indicated that the prospect lost about 3,536 MWt naturally to the atmosphere with 2440 MWt being the convective component (Mwawongo, 2005). Borehole geology indicates that the subsurface stratigraphic structure of the Menengai caldera consists of main rock units, inherited from the evolution history of the caldera, they include Pyroclastic, Tuff, Trachyte and Syenite(Figure 2). An upflow of high temperature fluid (above 300^{o}C) arises beneath the Menengai caldera through buried structures and is manifested at the surface by fumaroles especially close to MW-15A. The geochemical analysis of the fumarolic gas discharges indicate a deep, high temperature reservoir between 280-320^{o}C from gas geothermometry (Njue and Kipngok, 2018). Two separate boiling zones at elevations between 1000 to 1500 m.a.s.l and 400 to 700 m.a.s.l were identified from hydrothermal alteration of minerals during well logging. According to Geotermica Italiana (1987), a large positive gravity anomaly in the central part of the caldera, was related to a dense body located at 3.5-4 km deep having a density of 2.8 g/cm^3, which could be the source of heat Lagat, (2011) thought the heat source for the system is a shallow magma chamber with a hot intrusive penetrating into the reservoir as illustrated in (Figures 2,3&4). Recharge of cold water is from the east, northeast of the geothermal field (Leat, 1984), the caldera wall and other minor structures within the caldera. The main structure is the caldera itself which is elliptical in shape presenting a ring structure which is thought to be disturbed by the Solai graben faults on the northeast end and a fracture system at the south-southwest end (Strecker et al., 1990; Lagat et al., 2010). Complex subsurface fractures and lithological contacts provide the permeability conduits for recharge and upflow. Probable fluid flows in the NW, W and NE directions from the upflow region, forming the outflow of the Menengai reservoir (Montegrossi et al., 2015). There is evidence that the Menengai geothermal field is highly fractured and permeable below 500 m indicated by intense alteration with calcite and pyrite abundance into the bottom of the well of MW-18A. Figure 3 shows the cross-section of the eastern part of the caldera drawn from existing data.

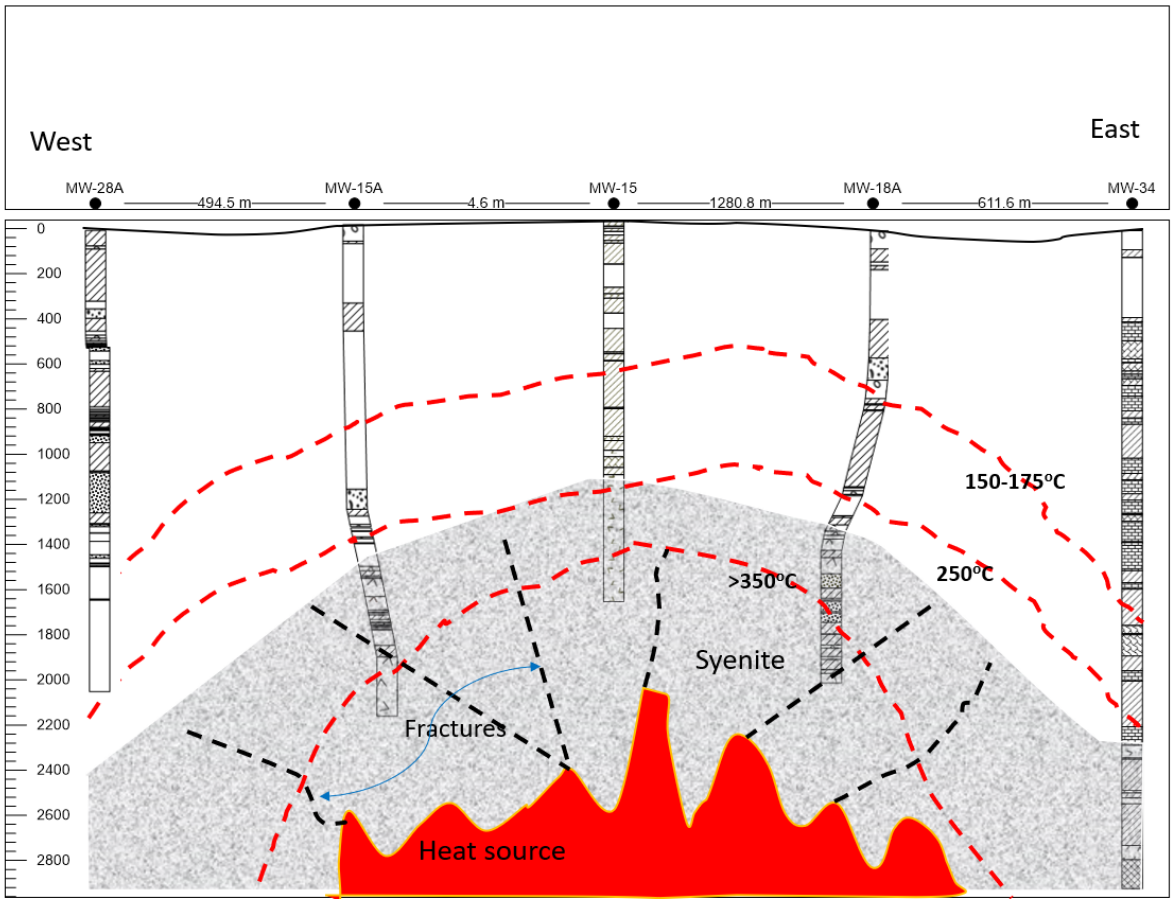

).

Figure 3:Shows the West-East geological cross-section model of Menengai East showing main up flow zone identified within the eastern part of the caldera as per the drilling results.

A conceptual model of the study area was developed to get a good understanding of the important aspects of the physical processes and structure of the geothermal system. The Conceptual model is obtained from geology, geochemistry, geophysics study results, and well data. It describes several vital components of a potential geothermal field, such as the heat source, natural fluid flow pattern, geological setting, caprock, upflow and outflow, and recharge zones. The area under consideration is located on the eastern part of the caldera, where the NNE Solai Graben cuts the caldera wall. To build the conceptual model, all the field data related to the area was compiled and analyzed. The Conceptual model is obtained from geology, geochemistry, geophysics survey results, and well data. The Conceptual model describes several information such as heat source, natural fluid flow pattern, geological setting, caprock, upflow and outflow zone and recharge. The conceptual model in this work was established according to the 700-2100 m fractured reservoir observed in MW-18A. The conceptual model components of the Menengai geothermal reservoir have previously been described by (Kipyego et al., 2013; O'Sullivan et al., 2015; Mibei et al.,2017) below is a summary of the conceptual considering input from the above mentioned.(Figure 4).

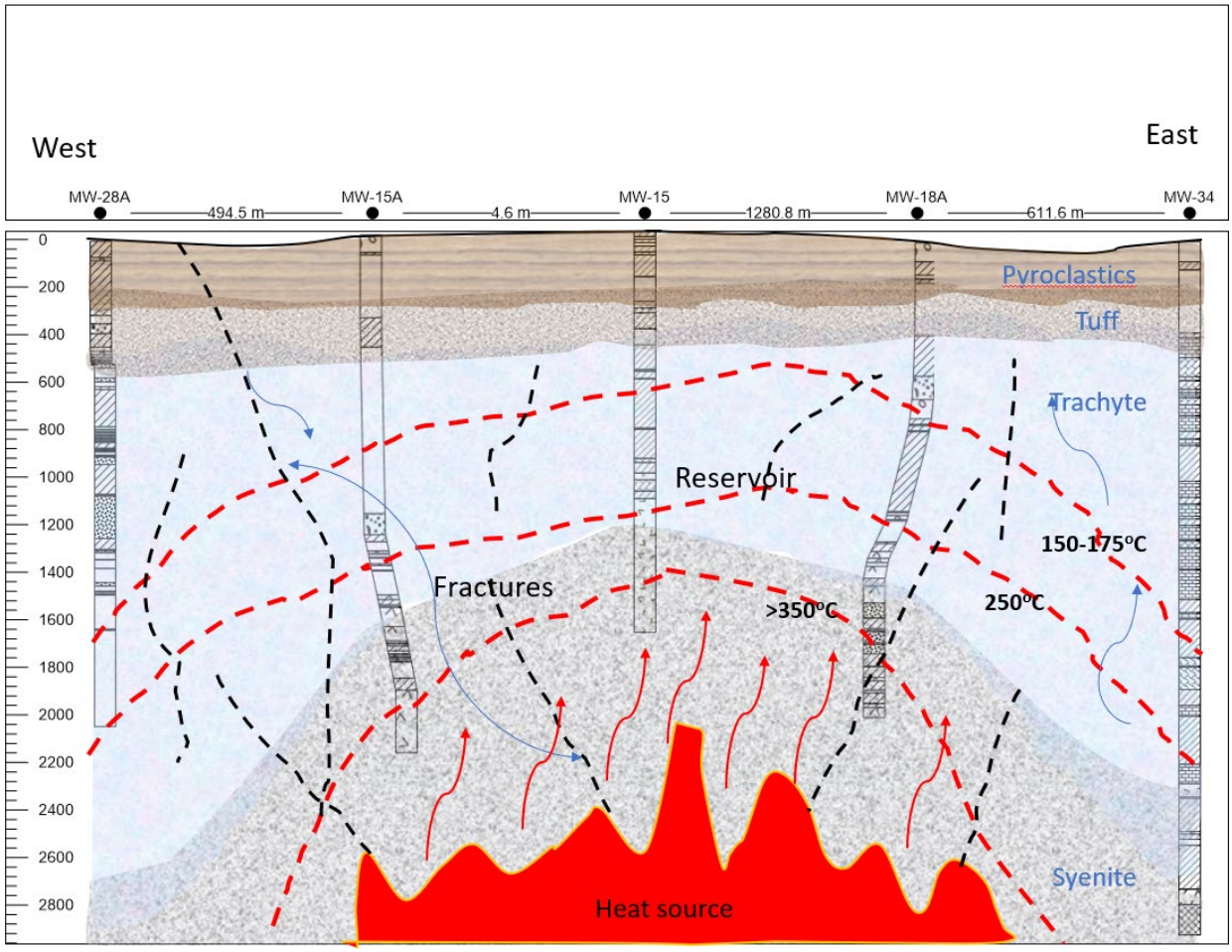

Figure 4: Shows the W-E conceptual temperature cross-section model of Menengai East showing the upflow on the Eastern part of the caldera.

2.0 Numerical and Simulation Approach

In this study, the natural state model of the Menengai East geothermal field was developed using TOUGH2 and built using the non-isothermal-pure water equation of state (EOS1). The Tough 2 V2.0 code was employed to navigate the coupled processes of fluid flow and heat transfer in the high temperature, naturally fractured geothermal reservoir. The code has previously been used as a numerical simulator for solving multiphase fluid and heat flows both in porous and fractured geological media (Pruess et al., 1999). When using this simulator, certain assumptions are made, such as the following: (1) Darcy's law is valid in the model domain, (2) the mechanical dispersion of dissolved gases is neglected, (3) the movement of the geologic medium is not described or taken into consideration, (4) when salts (dissolved components) are considered or are preset the aqueous phase cannot evaporate or disappear .

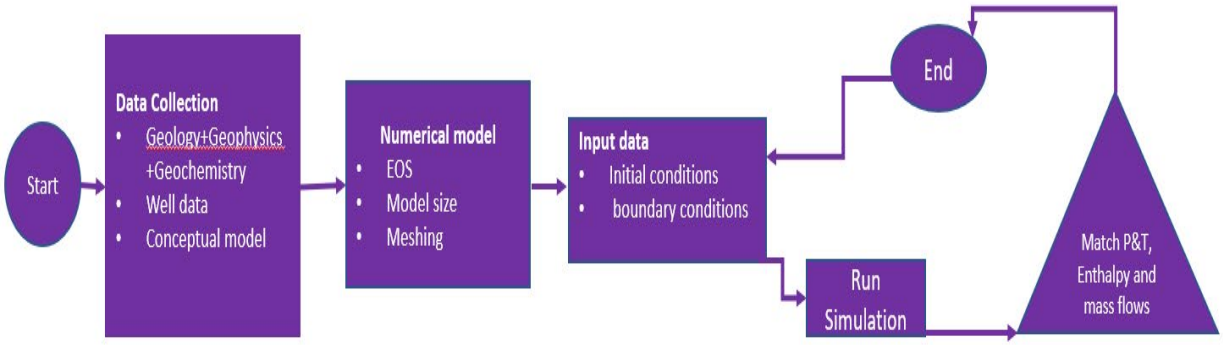

.

Figure 5: shows the steps followed in constructing a numerical model.

As summarized in figure 4, the following steps were followed in coming up with the numerical model. 1) We established the modeling goal and created a conceptual framework for the study, we built a conceptual model of the study area using data on the site's geology(structural and borelole), geophysics, geochemistry, and any other relevant information.

2) By establishing the boundary conditions and material attributes, we were able to determine the relevant theoretical models. As we iterated through the modeling process, we changed certain components.

3) The field was divided into an infinite number of distinct cells. This allowed us to transform the continuous problem into a discrete issue that could be resolved quantitatively.

4) The numerical model was subsequently put into practice, and it was confirmed using production data from drilled wells in this part of the field.

2.1 Numerical geometry and spatial discretization

The numerical model covers a 30.8 km^2 area between 173600 and 178800 E and 9975700 and 9979100 N. The surface model's maximum elevation is 1965 meters above sea level, and its lowest point is -1500 meters below sea level. Five geological layers with varied porosity have been used to build the model, which was laid out in a rectangular grid. The model has been divided into the five rock types identified in Menengai geothermal field, namely the base (syenite), caprock (trachyte), reservoir (pyroclastics), surface (pyroclastics), and magma (heat source). The reservoir is on average 2100 meters thick(NB it's not uniform because of the intrusive); the base(intrusive), is 400 meters thick is also not uniform its thicker at the center; the surface layer is 200–265 meters thick, and the caprock is up to 400 meters thick. 8,600 elements or blocks make up the entire system; the higher symmetry was considered because it can speed up the processing of the numerical model domain (Pruess et al., 1999; Pruess 2006). Figure 6 displays a 3D image of the model and the well locations, the table 1 lists the spatial discretization. 1

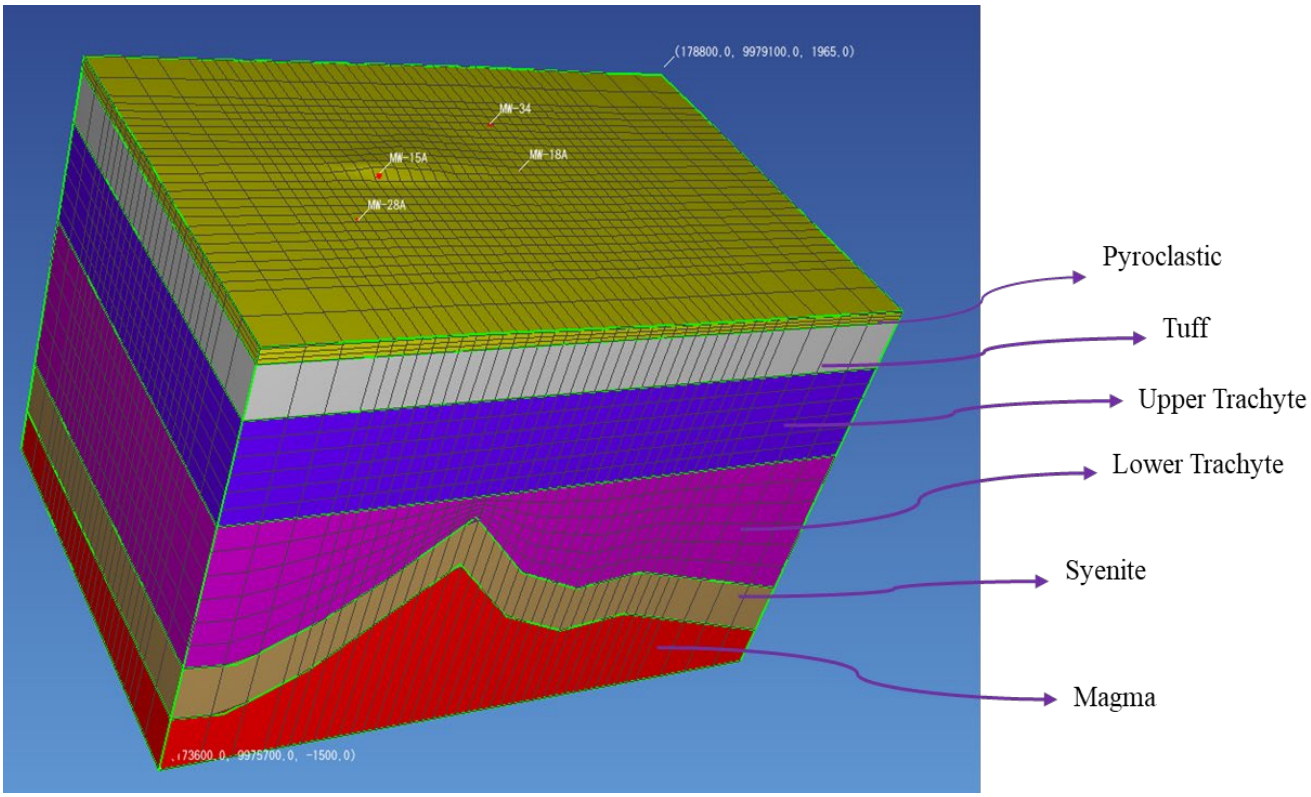

Figure 6: Shows the numerical model grid.

Table. 1 Model spatial discretization grid mesh

Direction	Cells	Cell size
X	2	300
X	2	250
X	33	100
X	2	250
X	2	300
Y	1	300
Y	1	250
Y	23	100
Y	1	250
Y	1	300

2.2 Initial and Boundary Condition

The atmospheric or surface layer is represented by the Top Layer. We are on the rift floor; thus, the allocated atmospheric conditions are 1 bar and 60ºC. To simulate the accurate location of the water table, the surface lithology is given a high permeability. The bottom barrier was given a high-temperature fluid recharge with an enthalpy of 1650 kJ/kg and a mass rate of 4.0E–5 kg/s.m^2.

Deep recharging takes place in the eastern part of MW-34. Based on the outcome of the calibration process, the recharge mass and heat flow and its location are established.

The initial hydrostatic pressure of well MW-18A increased from 6 MPa at a depth of 800 m to 14 Bar at the bottom of the fracture reservoir, i.e.,1800 m, according to well logging data, the initial reservoir temperature was uniform and had a value of 250°C. Because of their symmetry, the lateral borders were intended to be closed for mass and heat flow. Because of their low porosities and impermeability, the Base (Syenite) and Cap rock (Tuff) were not considered in the mass transfer with top and bottom boundaries. A semi-analytical method was used to assess the vertical exchange of the confining layers. The method signifies the temperature profile in a semi-infinite conductive layer by means of a simple trial function and shows reliable simulation accuracy (Pruess et al., 1999).

A deep fractured reservoir in Menengai that is primarily composed of trachyte is present at a depth between 600 and 2100 m (Figure 6), in addition there's a massive intrusive body in the central part of the reservoir as per the geological well logging results (Figures 3 and 4). It is thought that geothermal fluids are trapped in tectonic fissures and fracture zones in rocks covered by impermeable tuff. Caldera rim faults, which aid in vertical recharge, and the NNE-SSW faults in the Solai graben are two permeability controls discovered through gravity studies (Gichira and Mohamud, 2021). The capacity of the rock to transfer fluids determines the permeability of a geothermal reservoir. We have modelled target reservoir to have an intrinsic permeability of approximately 1–25 mD (1 mD = 1.0×10−15 m^2), such that only low-level stimulation (e.g., low-pressure, and short-term reservoir stimulation)will be required to initiate production.

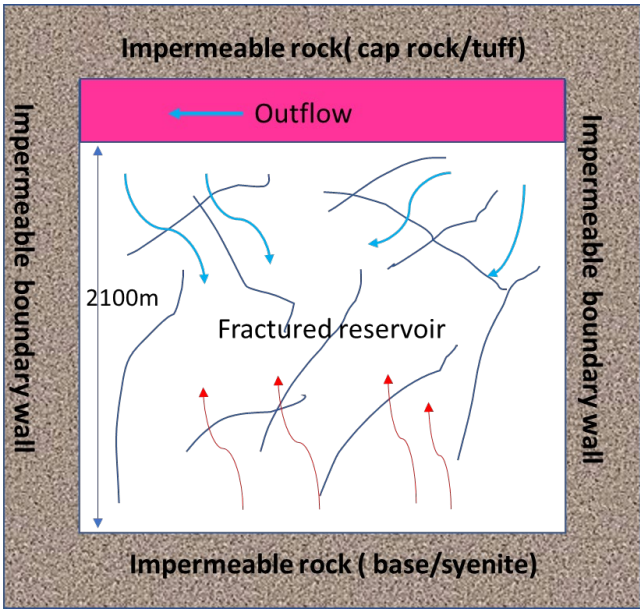

Figure 7: Illustrates an idealized fractured reservoir.

Our model is no-flow for mass and heat transfer with four boundary walls that do not allow any possible communication with the outside as illustrated in Figure 7. We have one major fracture to the east which represents the caldera wall which allows deep recharge into the reservoir, recharge takes place along the borders of the caldera, associated with the presence of major structures, which may favor the deep infiltration of meteoric water, with minor contribution from the magmatic system in the form of steam and gas.

2.3 Reservoir and Model properties

The reservoir properties and model parameters of the deep fractured geothermal reservoir in the eastern part of the caldera are given in Table 2. In the natural state modelling, the selection of material attributes plays a critical role. The most important property to give the best match in the natural state calibration process is permeability. Permeability will affect pressure and temperature distribution as well as the fluid movement direction in model. Therefore, permeability is given in the X,Y and Z direction. The permeability value ranges from 3.0E-14 to 9.86E-19 m^2 other material properties such as density, specific heat and wet heat conductivity are specified to 2900 kg/m^3, 1000 J/(kg^{o}C) and 4 W/(m.^{o} C) respectively. Permeability of rocks guided by the interconnectivity of pores within a rock matrix. Pore spaces must be interconnected and filled with water for fluid to be conducted. Therefore, porosities in our model range from 0.05-0.5.

Table 2: Reservoir properties and model parameters

Material	Density Kg/m^3	Perm X	Perm Y	Perm Z	Cond W/(m.^{o} C)	Porosity	Thickness(m)	Specific heat J/(kg.k)
Pyroclastic	2500	2.0E-15	2.0E-15	6.0E-15	2.0	0.01	200	1000
Tuff(Cap rock)	2670	6.0E-17	6.0E-17	6.0E-18	2.0	0.02	400	1000
Upper Trachyte	2600	2.5E-15	4.0E-15	1.0E-15	2.1	0.5	800	1000
Lower trachyte	2640	4.9E-15	4.9E-15	1.5E-15	2.1	0.3	1300	1000
Syenite(Basement)	2700	2.0E-17	2.0E-17	6.0E-17	3.5	0.05	400	1000
Magma	2800	9.0E-18	9.0E-18	9.0E-18	4.0	0.01	400	1000
Aquifer	2650	3.0E-14	3.0E-14	3.E-14	2.1	0.1	166	1000
Boundary	2900	9.86E-19	9.86E-19	9.86E-19	0	0.05	300	1000
Fracture	2500	3.95E-15	3.95E-15	3.95E-15	1.0	0.2	300	1000

Table 3: Operationalization of the Model parameters

Initial Temp ^{o} C at the top of reservoir	60^{o}C
Initial Pressure the top of reservoir	1Bar
Initial Liquid saturation	1
Source Sink	1.650E6J/Kg at rate of 4.50E-5kg/s

The cap rock and base rock were impermeable with the initial permeability of 6.0E-17 to prevent the recharge of fluid, but the heat exchange was calculated with the heat conduction efficiency of 3.5 W/(m ◦C).

3.0 Numerical validation

During the natural state process, the model was run until a steady state condition was reached. Several validation processes have been used to check the reliability of model, such as pressure and

temperature matching, steam zone presence, and heat and mass flow direction. To obtain a good fit between the model and actual measurements, several steps were taken using an iterative process such as a change in permeability and porosity values, determining the amount and enthalpy of deep mass recharge, adjustment on dimension, the location of source sink and block refinement using a new rock type to improve matching process. The final calibrated model reasonably reflects the conceptual model. Similar temperatures are shown in the natural state model especially those beneath MW-15A to those interpreted for the conceptual model.

Based on the conceptual model a 3D numerical natural state model was developed. The model was calibrated using try and error method based on available data from natural state conditions of reservoir to obtain a good match. During the natural state process, the model was run until a steady state condition was reached.

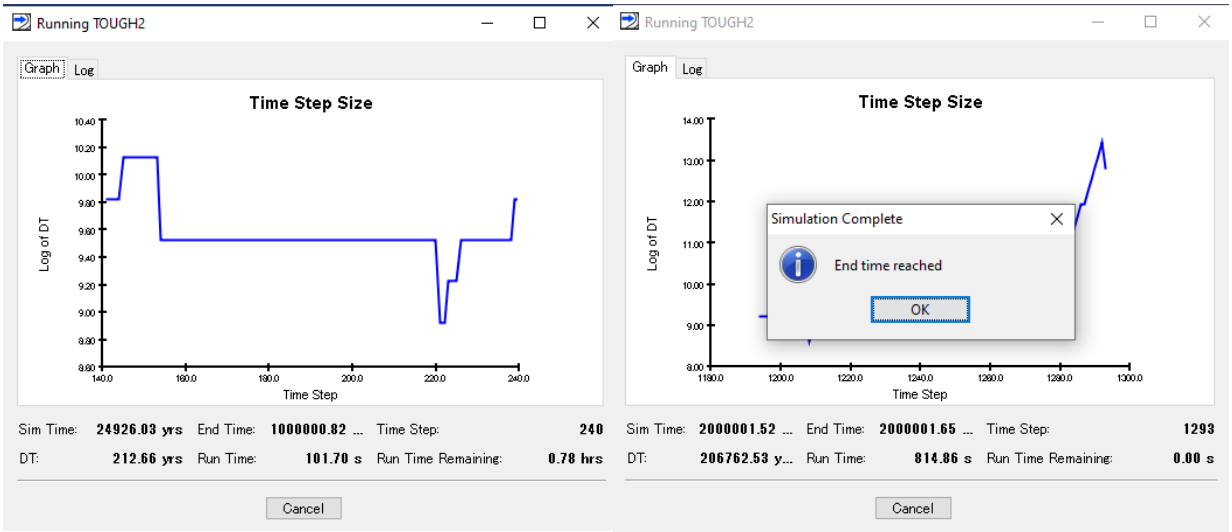

Figure 8: Shows the model running and end time reached after simulations.

Several validation processes have been used to check the reliability of model, such as pressure and temperature matching, steam zone presence, and heat and mass flow direction. To obtain a good fit between the model and actual measurement, several steps were enacted using an iterative process such as a change in permeability and porosity values, determining the amount and enthalpy of deep mass recharge, adjustment on size the location of source sink and block refinement using a new rock type to improve matching process.

The pressure and temperature of model are validated using 2 wells in Menengai MW-15A, MW-MW-18A (Figures 9 and 10) show the comparison between the model and measured data, the figures also show a prediction of deeper reservoir pressure and temperature profile. The figures show the contrast between the modeled and measured data, the figures also show a prediction of deeper reservoir pressure and temperature profile. The pressure and temperature matching of all wells give reasonable match for MW-15A and MW18A (Figures 9 and 10) .

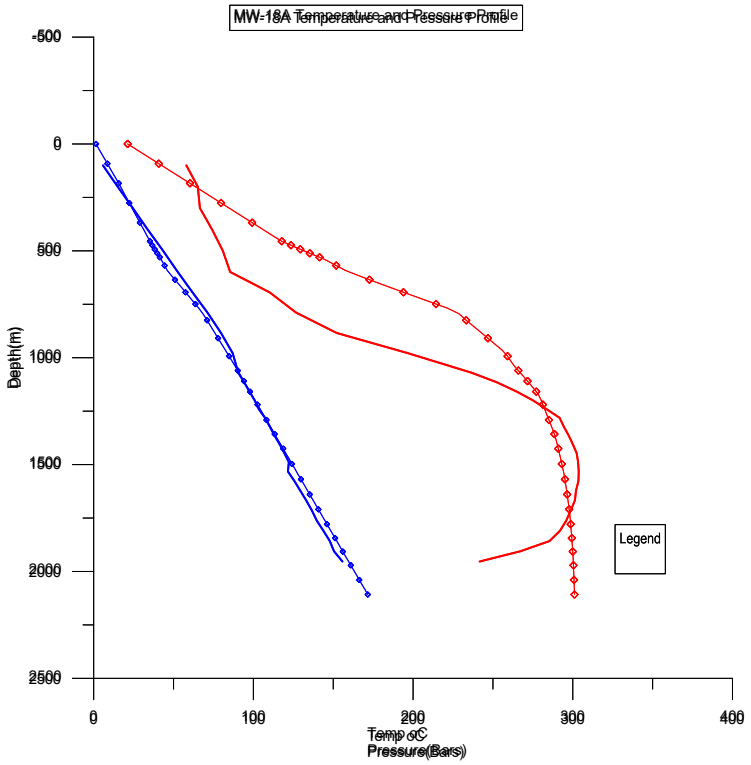

Figure 9: Shows the MW-18A temperature and pressure profiles from the Well, the initial model, the results.

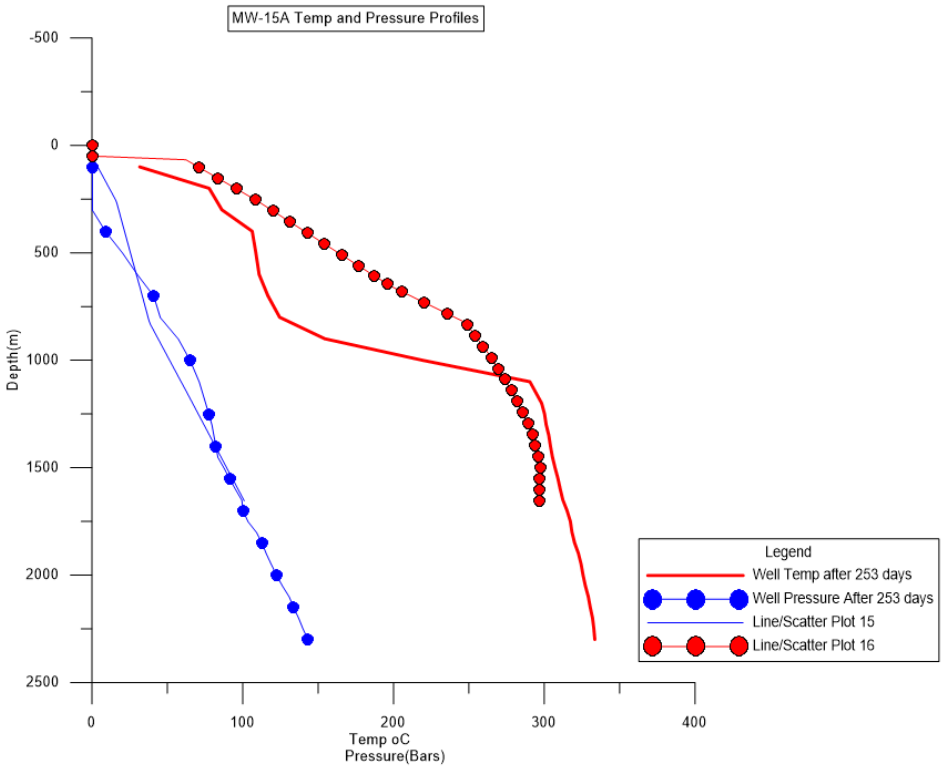

Figure 10:Shows the MW-15A temperature and pressure profiles from the Well, the initial model, the results.

4.0 Discussion and Conclusion

The natural state model of Menengai East, has been developed successfully. The Model has been able to reproduce shallow (steam reservoir) and deep reservoir condition (brine reservoir). The output of the natural state model has been validated using 2 wells of the actual measurement data also heat and mass flow from the conceptual model (Figures 9 and 10) give a reasonable match. The Model simulation has been able to reproduce shallow (steam reservoir) and deep reservoir condition (brine reservoir). The pressure and temperature in the shallow reservoir show a steam static pressure and convective temperature profile near saturation which is indicative of a steam dominated reservoir. The steam static pressure in the vapor reservoir occurred due to the equilibrium mass flux of steam moving up and water as the condensed steam moving down. All wells in the Eastern part of the caldera show a convective profile, the reservoir in Menengai east has the thickness range from 700-2000 m.

5.0 Acknowledgements

I sincerely appreciate the opportunity granted me to undertake this research by Geothermal Development Company and the support by JICA. I also want to thank my Co-Author Prof. Fujimitsu for his guidance.

6.0 References

Enerdata Kenya energy report, 2020: https://www.enerdata.net/estore/country-profiles/kenya-energy-report-enerdata

Gichira, J., and Mohamud, Y., 2021: Identification of permeability controls in a geothermal system using gravity method, Menengai Case study. Proceedings, world geothermal congress 2021,Reyjavik, Iceland.

Jung Y.,Pau,G.S.H., Finsterle,S., and Doughty C., 2018: TOUGH3 User's Guide Version 1.0

Kipyego, E., O'Sullivan, J. and O'Sullivan, M.,2013: An initial resource assessment of the Menengai caldera geothermal system using an air-water TOUGH2 model, Proceedings, 35th New Zealand Geothermal Workshop, Rotorua, November 18-20, (2013).

Lagat, J., Mbia, P., and Muturia, C.L., 2010: Menengai prospect: Investigations for its geothermal potential. Contributions from: Njue, L., Mutonga, M., Malimo, S., Kanda, I., Kipngok, J., Mwakirani, R., Suwai, J., and Mutie, T. Geothermal Development Company - GDC, Kenya, Geothermal Resource Assessment Project, 57 pp

Mibei,G., Mutua,J., Kahiga,E, and Lopeyok,T., 2017: The use of Leapfrog software in Geothermal modelling; case study of Menengai Geothermal Field Corpus ID: 201648806

Montegrossi G., Pasqua C., Battistelli A., Mwawongo G. and, Ofwona C.,2015: 3D Natural State Model of the Menengai Geothermal System, Kenya, Proceedings World Geothermal Congress 2015 Melbourne, Australia, 19-25 April 2015

Mwawongo, G.M., 2005: Kenya's geothermal prospects outside Olkaria: Status of exploration and development. Lecture 4 in: Mwangi, M.N. (lecturer), Lectures on geothermal in Kenya and Africa. UNU-GTP, Iceland, Report 4, 41-50.

Njue L., & Jeremiah Kipngok J., 2018: Menengai Geothermal Field Eastern Upflow Proceedings, 7th African Rift Geothermal Conference Kigali, Rwanda 2018

O'Sullivan, JO., Kipyego, E., Adrian Croucher, A., Ofwona, C., and O'Sullivan, M., 2015: A Supercritical Model of the Menengai Geothermal System

Pruess, K., 2006: Enhanced geothermal systems (EGS) using CO^2 as working fluid - A novel approach for generating renewable energy with simultaneous sequestration of carbon. Geothermics 35 (4), 351–367.

Pruess, K., Oldenburg, C.M., Moridis, G.J., 1999: TOUGH2 User's Guide Version 2. Lawrence Berkeley National Lab. (LBNL), Berkeley, CA (United States), p. Medium:

Simiyu, S.M., and Keller, G.R., 1997: Integrated geophysical analysis of the East African Plateau from gravity anomalies and recent seismic studies. Tectonophysics, 278, 291-314

Strecker, M.R., Blisniuk, P., and Eisbacher, G., 1990: Rotation of extension direction in the Central Kenya Rift. Geology, 18, 299–302.